A Primal Dual Interior Point Framework for EIT Reconstruction with Automatic Regularization

Yasin Mamatjan[1], Andrea Borsic[2], Doga Gürsoy[3] and Andy Adler[1]
[1] Systems and Computer Engineering, Carleton University, Ottawa, Canada
[2] Thayer School of Engineering, Dartmouth College, USA
[3] Department of Physics, University of Houston, USA

***Abstract*—The spatial resolution of the reconstructed images in Electrical impedance tomography (EIT) is low and a priori information regarding smooth conductivity changes limits reconstruction of sharp images while it is preferred in order to differentiate tissue boundaries in medical imaging. Measurement errors are another barrier that hinder a good image reconstruction. Generally ℓ_2 norms have been used due to computational convenience both for data and regularization terms which result in smooth solutions. However, the recent developments in optimization problem the Primal Dual-Interior Point Method (PDIPM) showed its effectiveness in dealing with the minimization problem. ℓ_1 norms on data and regularization terms in EIT image reconstruction address both problems of reconstruction with sharp edges and dealing with the electrode errors.**

We demonstrated general formulation of the Primal-Dual Interior Point framework for EIT image reconstruction. We systematically evaluated the PDIPM algorithms with ℓ_1 and ℓ_2 norm based minimization in EIT inverse problems with automatic regularization based on a balancing principle. The performance of algorithms was evaluated in 4 scenarios in simulation. Finally we demonstrated its applicability for medical EIT through results from dog breathing experiments. The results show that the ℓ_1 minimization for EIT image reconstruction produced sharp edge and proved to be robust against measurement errors.

I. Introduction

Electrical Impedance Tomography (EIT) is a non-invasive and non-ionizing imaging modality that aims to reconstruct the passive electrical properties in a conducting body. Pairs of electrodes are consecutively used to generate different current density distributions within the body. For each current excitation, the remaining electrodes are used to measure the electric potentials on the surface. The measured potentials are then used to reconstruct the cross-sectional conductivity and permittivity images of the body. Currently, EIT has shown the most promising clinical application in intensive care units (ICU) by monitoring the distribution of inspired air in mechanically ventilated patients. Such ventilation can often result in ventilator-associated lung injuries and EIT can resolve changes in the distribution of lung volume between dependent and independent lung regions as ventilator parameters are changed and consecutively minimize the risk of a potential lung injury related to the ventilation pressure.

Image reconstruction in EIT is an ill-posed inverse problem. The spatial resolution of the reconstructed images is low and limited due to the small number of measurements and highly underdetermined system of equations. The sensitivity matrix is ill-conditioned that measurement noise usually leads to large artefacts in the images unless regularized appropriately. In order to maintain image stability and meaningful images, regularization techniques are employed to reduce these artefacts. A priori information typically assumes smooth conductivity changes that limits reconstruction of sharp images. However, sharp edges are physiologically more realistic considering organ boundaries and reconstruction of edges can yield more reliable and clinically useful images. To reconstruct sharp edges, several techniques have been recently adapted to EIT by recovering discontinuous conductivities using Total Variation (TV), topology reconstruction via level-set, linear sampling methods [1] and Level Set method for EIT lung images. These approaches have been proved to be useful for solving problems with sharp conductivity transitions.

The inverse problem requires minimization of a cost function which typically consists a data fidelity and a regularization term. Generally the ℓ_2-norm is preferred due to its computational convenience for both terms and results in smooth solutions. However, use of ℓ_1-norm is known to promote sparsity and piecewise constant solutions based on the regularization type. On the other hand, ℓ_1-norm on the data fidelity term works well when the measurements are contaminated by impulsive noise. The use of ℓ_1 and ℓ_2 norms for both the data

and regularization terms were formulated for the EIT problem based on the Lagged Diffusivity Method (LDM) by Dai and Adler [2]. They used a weighted identity matrix for regularization which promotes the sparsity.

The choice of regularization in general determines the constraints to the solution. Dai and Adler [2] used a weighted identity matrix for the regularization which promoted sparse solutions and suppressed the background fluctuations in the images. On the other hand, TV regularization is better adapted for piecewise smooth distributions. Borsic [1] highlighted the importance of TV regularization for EIT and compared the two different implementations of the TV functional, that is LDM and the Primal Dual-Interior Point Method (PDIPM). In the solutions of both methods, the so called staircase effect can be noticed in the reconstructed images.

In this paper, we perform a comprehensive study to compare and evaluate the PDIPM framework using ℓ_1 and ℓ_2 norms for both the data-fidelity and regularization terms. We performed our simulations using synthetic datasets for 4 different scenarios. The real-measurements include datasets from dog breathing. A systematic approach for regularization was also investigated and an automatic regularization based on the Balancing principle is implemented. Finally, we made analysis and compared these four methods in this framework.

II. Methodology

A. EIT inverse problem

In EIT, the measurements (data) are the surface potentials on the boundary of the object and are discrete. Let $f(\mathbf{x}) = \mathbf{y}$ represents the nonlinear relationship between the data (voltage data) and model parameters (electrical properties), $\mathbf{x} : \mathbf{x} \in R^N$ and $\mathbf{y} : \mathbf{y} \in R^M$, respectively. Generally, the number of the unknown model parameters are much more than the available number of data, $i.e., M < N$, which results in an underdetermined set of equations. The corresponding inverse problem of recovering $\mathbf{x}$ from $\mathbf{y}$ based on the mapping f can be stated in the form of a minimization problem as follows:

$$\arg\min_{\mathbf{x}} \left\{ \mathcal{F}(\mathbf{x}) := ||f(\mathbf{x}) - \mathbf{y}||_p + \lambda ||\mathbf{R}(\mathbf{x} - \mathbf{x}_0)||_n \right\}, \tag{1}$$

where the $||f(\mathbf{x}) - \mathbf{y}||_p$ is the data fidelity term and $||\mathbf{R}(\mathbf{x}-\mathbf{x}_0)||_n$ is the regularization term, and $\mathbf{x}_0$ is a prior conductivity distribution (in our case the initial estimate was set to zero); $\mathbf{R} : \mathbf{R} \in R^{M \times N}$ is usually referred to as the regularization matrix and constructed based on the a priori information about the model parameters. The trade-off between these two terms is determined by the regularization parameter λ. p and n respectively specifies the types of norms for the data fidelity and regularization terms. The characteristics of the solutions are dependent on the choice of the norms. The detailed descriptions of different norms can be found in [3].

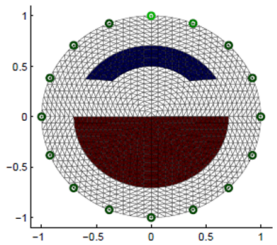

Fig. 1. Image of the 2D phantom with two inclusions used for generating the simulated data based on finite element model.

B. Experimental data

A typical EIT system with adjacent stimulation and voltage measurement was considered for both the simulation and experimental evaluations, and 16 electrodes were arranged on one electrode plane in a circular pattern. Current is injected between an adjacent pair of electrodes and voltages are measured between all other adjacent pairs to avoid the error due to the contact impedance.

1) Simulation: The forward model employed in this study was a circular finite element model (FEM) which was implemented using EIDORS [4]. Fig. 1 shows a 2D phantom used for generating simulated data (2304 elements). The phantom presents two sharp inclusions in the upper and lower regions.

The background conductivity value is 1 S/m, the top inclusion presents a value of 0.5 S/m and the bottom inclusion a value of 1.5 S/m. Electrodes were indicated by green dots around the circular phantom. To avoid the *inverse crime*, the reconstructed images used different mesh (576 elements) to make it different from the forward computations.

To analyze the performance of the PDIPM framework, following scenarios were simulated based on: (A) original numerical phantom, (B) added noise which is formed by adding zero mean Gaussian noise to the simulated measurements to give an SNR of 60 dB which is reasonable for most EIT systems, (C) a data error (outlier) which was introduced to the data randomly, (D) adding noise and a data outlier.

Furthermore, measurement outliers were introduced as a type of electrode-error to test the robustness of the proposed algorithms for certain electrode malfunction with a measurement failure rate of 0.5% to 15% (1 to 30 measurement indices out of 208 for one frame). 1 to

30 measurement outliers are added to the EIT data for randomly generated indices (Matlab randint function).

C. Adaptive choice of regularization parameter

The optimal choice of the regularization parameter λ can be found according to the balancing principle:

$$(\sigma - 1)||f(\mathbf{x}_\lambda) - \mathbf{y}||_p + \lambda||\mathbf{R}\mathbf{x}_\lambda||_n = 0, \qquad (2)$$

where $\sigma : \sigma > 1$ is introduced to balance the data fidelity and the regularization terms to determine the trade-off between them. In here, the dependency of the solution on the regularization parameter is represented by an additional subscript. A similar balancing idea commonly underlies ℓ_2-ℓ_2 formulations, for instance the local minimum criterion, zero crossing method or the L-curve criterion. According to equation (2), the regularization parameter λ can be calculated means to the following fixed point iteration:

$$\lambda_{k+1} = \frac{T||f(\mathbf{x}_{\lambda_k}) - \mathbf{y}||_p}{||\mathbf{R}\mathbf{x}_{\lambda_k}||_n} \qquad (3)$$

where $T = \sigma - 1$.

D. Experimental evaluation

A 16-electrode EIT system was used to take measurements of conductivity changes due to lung ventilation and lung fluid instillation in mongrel dogs [5]. Measurements were taken before and after 100 ml of fluids (5 % bovine albumin and Evans blue dye) were injected to a lobe of the right lung at the presence of 700 ml inspiration. The data before fluid instillation was used as reference data for the subsequent measurements right after fluid injection and 60 minutes after the fluid injection. The data were known to contain electrode errors from previous work [5].

III. RESULTS

Fig. 2 shows a set of simulated result using PDIPM algorithm with $\ell_2\ell_2$, $\ell_1\ell_2$, $\ell_2\ell_1$ and $\ell_1\ell_1$ under 4 test scenarios: (A) without noise in row 1, (B) noise (-60 dB) in row 2, (C) 1 outlier in row 3 and (D) both noise and 1 outlier in row 4. λ was selected from the minimum RMS value and they were fixed from test1 to test 4 scenarios for all corresponding ℓ of data and regularization terms. The selected T values were $4.096 * 10^{-2}$, 10^{-2}, $1.25 * 10^{-3}$ and $1.728 * 10^{-2}$ respectively for for $\ell_2\ell_2$, $\ell_1\ell_2$, $\ell_2\ell_1$ and $\ell_1\ell_1$.

It can be seen from Fig. 2 that all algorithms provide reasonable reconstructed images for without noise scenario (row 1), but under noise (row 2) but under noise (row 2), the reconstruction quality drops. For the case

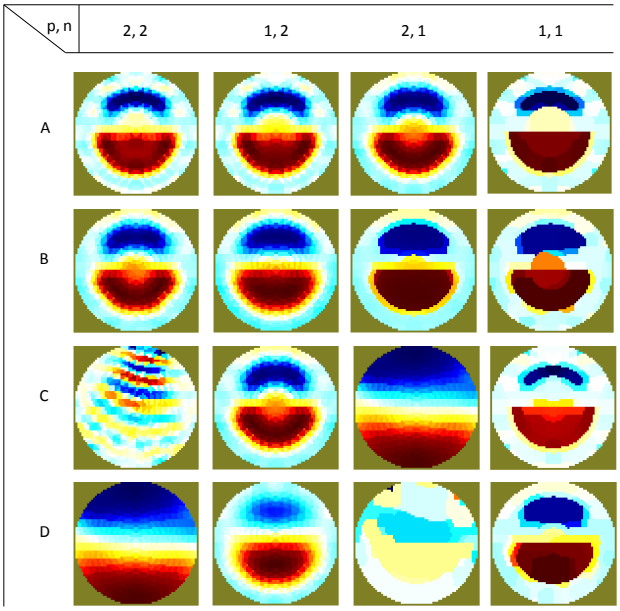

Fig. 2. Reconstructed images using PDIPM algorithm with $\ell_2\ell_2$, $\ell_1\ell_2$, $\ell_2\ell_1$ and $\ell_1\ell_1$ under 4 test scenarios: (A) without noise in row 1, (B) adding noise in row 2, (C) presence of one strong outlier in the dataset in row 3 and (D) both the presence of noise and one strong outlier in row 4.

of ℓ_2 regularization, the images gets blurry and for ℓ_1 regularization, several artefacts appear on the images. When an outlier is considered (row 3 and 4), $\ell_2\ell_2$ and $\ell_2\ell_1$ fail to work while $\ell_1\ell_2$ and $\ell_1\ell_1$ algorithms were pretty robust at the presence of one data outlier.

There are two tuneable parameters σ and α. The choice of value of σ balance the data fidelity and regularization terms to determine the trade-off between them using the balancing principle as in eq. 20. α is initial regularization parameter and the regularization parameter estimation iterated 5 times.

We used generalized balancing principle by [6] and adapted it for all combinations of ℓ_1 and ℓ_2 for simulation and experimental evaluations. We compared the performance of generalized estimation (Balancing principle) approach with the parameters chosen empirically for the best comprise between image resolution and noise performance. The balancing principle based approach calculates regularization parameters automatically, which works as a calibration parameter that can be automatically calculated for different sequence of data in the same scenario. Although we have test and find better sigma values for different scenarios and ℓ types, it is more efficient than hand selected approach where a great range of values has to be tested and which is different for different sequences of data or scenario.

The performance of PDIPM algorithms was further evaluated based on the measurement data with electrode

errors. Fig. 3 illustrates the use of PDIPM algorithms for imaging the conductivity changes in dog's lung immediately after fluid injection (row 1) and 60 minutes after the fluid injection (row 2) with the presence of certain level of electrode errors.

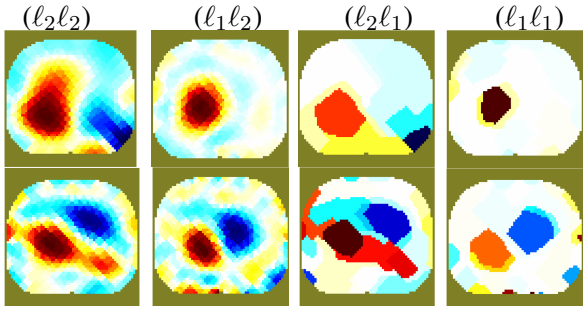

Fig. 3. Reconstructed cross-section of conductivity changes in dog's lung right after fluid injection (row 1) and 60 minutes after the fluid injection (row 2). Difference images were reconstructed using PDIPM algorithms, where the presence of electrode errors in the measured data affected all terms except $\ell_1\ell_1$.

As shown in the cross-sectional images in Fig. 3 that $\ell_2\ell_2$ is suffered the most from noise from measurement system. Thus, $\ell_1\ell_2$ and $\ell_1\ell_1$ are good candidates for the reconstruction based on real measurement data. They complement one another to look at the two sides of the same data with sharp and smooth edges.

The PDIPM algorithms showed their dependence on σ values. For simulation, initial hyperparameter α does not much effect the estimation of good hyperparameter. It is found from the experimental evaluation that choice of σ varies depending on application.

IV. DISCUSSIONS AND CONCLUSIONS

In this study, we introduced PDIPM frame work for EIT inverse problems and investigated PDIPM algorithms in simulation and real-measurement using 4 combinations of ℓ_1/ℓ_2 norms on data and regularization terms. To compare those algorithms systematically 4 test scenarios were evaluated. We used balancing principle to automatically choose regularization parameters. We also evaluated the PDIPM algorithms with real-measurement on dog breathing.

The test studies based on Fig. 2 showed that $\ell_1\ell_2$ and $\ell_1\ell_1$ are not affected by data outliers because of 1-norm for the data term without squared difference between the model and actual data, while $\ell_2\ell_1$ and $\ell_1\ell_1$ produces sharper reconstructed images because of 1-norm on the regularization term which is not overly-penalized. $\ell_1\ell_1$ provided both sharp conductivity image and robustness to data outliers.

Gauss-Newton based 2-norm solutions have been used frequently as established traditional method. However, PDIPM algorithms with 1-norm ($\ell_1\ell_1$) are particularly important in medical applications of EIT, since in reality, noise from the acquisition system, and electrode movements or electrode errors are unavoidable, which greatly affect reconstructed image quality based on the 2-norm (data term) solution.

$\ell_2\ell_2$ is more sensitive to data outliers and also produces blobby images since it filters out noise as well as useful information. Nevertheless, $\ell_2\ell_2$ takes least computation time since the NOSER algorithm was used in the first iteration which is also widely used in EIT imaging. $\ell_2\ell_1$ is computationally the most costly for less than 10 iterations.

The traditional image reconstruction is based on ℓ_2 norm, which basically produces smooth solution without any clear edge and is sensitive to measurement noise. ℓ_1 penalty for a data outlier is smaller than ℓ_2 which squared the differences, so ℓ_1 solution is less prone to measurement errors. However, ℓ_1 solution is not efficient compared to traditional Gauss-Newton based solution, since ℓ_1 solution involves with the minimization of a non-differentiable function, thus requires more computation time and more iterations to reach the convergence.

This paper brought an insight and useful analysis on PDIPM framework, which is well suitable for clinical EIT where noise from environment, subject and instruments have serious effects on the practical application of EIT. ℓ_1 solution shows shaper conductivity profiles that are closer to the model conductivity distribution and ℓ_1 solution is also more robust to data outliers.

REFERENCES

[1] A. Borsic, B. Graham, A. Adler, and W. Lionheart, "In vivo impedance imaging with total variation regularization," *IEEE Trans. Med. Imaging*, vol. 29, pp. 44–54, 2010.

[2] T. Dai and A. Adler, "Electrical impedance tomography reconstruction using l1 norms for data and image terms," *IEEE EMBC*, pp. 2721–2724, 2008.

[3] A. Borsic and A. Adler, "A primal dual - interior point framework for using the l1-norm or the l2-norm on the data and regularization terms of inverse problems," *Submitted to Inverse Problems*, January, 2012.

[4] A. Adler and W. Lionheart, "Uses and abuses of eidors: An extensible software base for eit," *Physiol Meas*, vol. 27, p. 25, 2006.

[5] A. Adler, R. Amyot, R. Guardo, J. Bates, and Y. Berthiaume, "Monitoring changes in lung air and liquid volumes with electrical impedance tomography," *J. Appl. Physiol.*, vol. 83, pp. 1762–1767, 1997.

[6] C. Clason, B. Jin, and K. Kunisch, "A duality-based splitting method for l1-tv image restoration with automatic regularization parameter choice," *SIAM J. Sci. Comput.*, vol. 32, pp. 1484–1505, 2010.